Characterization of polymeric materials for solar-thermal collector mounting systems

Joerg Fischer[1], Patrick R. Bradler[1], Sandra Leitner[1], Gernot M. Wallner[1] and Reinhold W. Lang[1]

[1] Institute of Polymeric Materials and Testing / Johannes Kepler University, Linz (Austria)

Abstract

In this research, three unreinforced and two glass fiber reinforced plastics for the application in mounting systems of solar-thermal collectors were investigated comprehensively. Therefore, morphological, thermomechanical, mechanical and cyclic fracture mechanical tests were performed. Focus was given on the mechanical properties and the fatigue crack growth (FCG) resistance at service relevant temperatures. In the morphological characterization, for the five materials primarily homogenous material distributions were detected. However, the polymer blend ASA/PC showed a limited miscibility. This was confirmed by the separated glass transition temperatures, which were determined by dynamic mechanical analysis. In terms of mechanical properties, significantly higher values for Young's modulus and strength as well as lower strain-at-break values were obtained for the glass fiber reinforced polymer grades. Increasing temperatures led to decreasing Young's moduli and strengths as well as to higher strain-at-break values. The unreinforced plastics revealed an inferior FCG resistance. For all materials, temperature increase evoked a declining FCG behavior. The FCG resistance of the reinforced plastics was influenced by the fiber orientation.

Keywords: plastics, solar-thermal collectors, mounting systems, mechanical properties, fatigue crack growth

1. Introduction and scope

Currently, mounting systems of solar-thermal collectors are constructed from aluminum or stainless steel (Erfurth et al., 2001; Koehl et al., 2012). For the reduction of costs and weight, it is a common practice to replace conventional materials with advanced polymeric material solutions. For an appropriate material replacement, various aspects must be carefully considered. Materials for mounting and framing must withstand environmental loads (e.g., temperatures, environmental media) and mechanical loads (e.g., weight of the mounted solar-thermal collector, snow weight, wind load, hail) (Erfurth et al., 2001; Koehl et al., 2012). The loading conditions can adversely affect the structural performance of polymeric materials (Altstaedt, 2005; DeCoste et al., 1951; Fischer et al., 2016a; Lang et al., 1997; Lang et al., 2005; Stern et al. 1998a; Stern et. al. 1998b). A comprehensive understanding of the material behavior under service relevant loading conditions is of utmost importance. Thus, previous research focused on the effect of superimposed mechanical and environmental loads on the properties of polymeric materials (Bradler et al., 2016; Bradler et al., 2017; Fischer et al., 2016a; Fischer J. et al., 2016a; Schoeffl and Lang, 2015).

The main objective of this research was the characterization of the morphological, thermomechanical, mechanical and fatigue crack growth (FCG) behavior of polymeric materials for mounting systems of solar-thermal collectors under application relevant temperatures. Therefore, infrared spectroscopic microscopy, dynamic mechanical analysis, monotonic tensile tests and cyclic fracture mechanics tests were performed at three different temperatures (0°C, 23°C, 60°C) in air environment.

2. Background

The linear elastic fracture mechanics concept was used for the investigation of the fatigue crack growth (FCG) behavior of plastics (Anderson, 2017; Bradler et al., 2016; Bradler et al., 2017; Fischer et al., 2016a; Fischer J. et al., 2016b; Lang, 1980; Schoeffl and Lang, 2015). In this concept, the fatigue crack growth rate (da/dN) is plotted against the stress intensity factor range ΔK. While the crack growth rate indicates the crack growth per cycle, the

doi:10.18086/swc.2017.31.03 Available at http://proceedings.ises.org

ΔK_I-value, described in eq. 1, is the difference between maximum and minimum stress intensity factor ($K_{I,max}$-$K_{I,min}$) of a cycling loading profile in loading mode I (pure tensile loads). In this equation, "$\Delta\sigma$" describes the global loading, "a" the crack length and "Y" a factor which is dependent on the geometry of the specimen used.

$$\Delta K_I = \Delta\sigma \cdot \sqrt{a} \cdot Y \tag{1}$$

In the double-logarithmic fatigue crack growth kinetics curve, region II represents the stable crack growth of the material. In a comparison of different polymeric materials or of different test conditions, improved fatigue crack growth resistance is revealed by a shift of the FCG curve to higher ΔK-values. Additionally, also slope decrease of the FCG curve exhibits improved FCG behavior (Haager, 2004; Lang, 2005).

3. Experimental

Materials

An overview of all investigated materials is given in Table 1, comprising three unreinforced and two glass fiber reinforced plastics. These materials were characterized with different methods at service relevant temperatures (0°C, 23°C, 60°C). The unreinforced polymer grades contain an acrylic ester-styrene-acrylonitrile copolymer (ASA), a polymer blend of ASA and polycarbonate (ASA-PC) as well as a polymer blend of polybutylene terephthalate and polycarbonate (PBT-PC). The reinforced plastics include a short glass fiber reinforced polyamide grade with a fiber content of 30 w% (PA-GF30) and a long glass fiber reinforced polyamide grade with a fiber content of 40 w% (PA-LGF40).

Tab. 1: Material designation and material composition.

Material designation	Material	Reinforcement type	Reinforcement content
ASA	Acrylic ester-styrene-acrylonitrile copolymer	-	-
ASA-PC	Polymer blend of acrylic ester-styrene-acrylonitrile copolymer and polycarbonate	-	-
PBT-PC	Polymer blend of polybutylene terephthalate and polycarbonate	-	-
PA6-GF30	Polyamide 6	Short glass fibers	30 w%
PA6-LGF40	Polyamide 6	Long glass fibers	40 w%

Infrared spectroscopic microscopy

To analyze the morphology and the fiber orientation within the compounds, the specimens were characterized with an infrared spectroscopic microscope PerkinElmer Spotlight 400 FT-IR Imaging System (Perkin Elmer Inc., USA. Tests were carried out with an attenuated total reflection mode (ATR). The spectral range was 650 cm^{-1} to 4000 cm^{-1}.

Dynamic mechanical analysis

Dynamic mechanical analysis (DMA) measurements were performed on an Anton Paar Physica MCR 502 (Anton Paar GmbH, Austria) for determining the temperature dependency of the storage modulus and the loss factor. The loss factor can be calculated out of the ratio between the storage modulus and the loss modulus. All DMA tests were conducted in a temperature range of -70°C and 220°C with a heating rate of 3 K/min. The applied frequency was set to 1 Hz and a torsional loading mode was applied. The samples were cut from the parallel part of the 1B multi-purpose specimen (ISO 527) with the dimension 40 mm x 10 mm x 4 mm.

Tensile tests

The mechanical properties (Young's modulus, strength and strain-at-break) were examined with a universal testing machine Z020 (Zwick Roell, Germany) equipped with a multi-extensometer and a temperature chamber for test at 0°C, 23°C and 60°C. Test parameters and multi-purpose specimens were used according to ISO 527 with a traverse speed of 1 mm/min for Young's modulus determination until a strain of 0.25 % and 50 mm/min until failure.

Fatigue crack growth

In order to investigate the fatigue crack growth (FCG) behavior, all five materials were tested with an in-situ testing device (Schoeffl et al., 2014) allowing fatigue tests at different temperatures within service-relevant environmental environments. Therefore, an electro-dynamic testing machine of the type ElectroPuls E3000 (Instron Inc., USA) was used. Compact type (CT) specimens with an initial crack in mold direction and in cross direction were utilized for investigations of the crack growth (Fischer et al., 2016b). A sinusoidal loading profile with a frequency of 5 Hz and an R-ratio of 0.1 was applied. Characteristic double-logarithmic FCG kinetic curves were plotted providing the relation between the FCG rate, da/dN, and the stress intensity factor range, ΔK_I, describing the local crack tip stress field.

4. Results and discussion

In the morphological characterization via infrared spectroscopic microscopy, for the two blends (ASA/PC and PBT/PC), a predominantly homogenous color distribution was found (see Fig. 1), with a limited miscibility of the ASA/PC blend. The reinforced grades revealed in the middle of the specimen a clear fiber orientation in cross mold direction. Conversely, due to higher shear loads, a fiber orientation in mold direction was found on the surfaces of the specimens. Fischer et al. reported this effect before (Fischer et al., 2016).

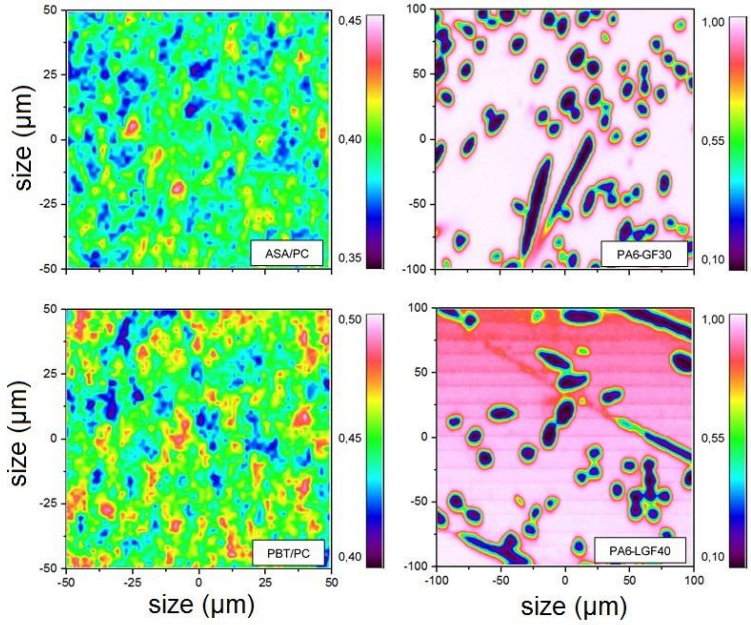

Fig. 1: Infrared spectroscopic map of the morphology of two polymer blends (left) and fiber orientation of two glass fiber reinforced polymers (right).

Curves of the storage modulus and the loss factor as a function of temperature (see Fig. 2) were attained via dynamic mechanical analysis (DMA). For the unreinforced materials, the highest storage moduli were exhibited for ASA and the lowest storage moduli for the PBT-PC blend. The glass transition temperature is depicted as a maximum of the loss factor curve. The ASA grade shows a peak at 124°C, for the ASA-PC compound two peaks are detectable, one for the ASA component at about 115°C, and a second at 149°C for the PC component. Hence, the limited miscibility obtained by infrared spectroscopic microscopy was assured. For the PBT-PC blend, a glass transition temperature of 140°C was found. The DMA data of the reinforced grades exhibit higher modulus values for the PA-grade PA6-LGF40 with 40 w% glass fiber reinforcement compared to the PA-grade PA6-GF30 with

30 w% glass fiber reinforcement. The glass transition temperatures of both PA-grades are similar (60°C for PA6-GF30 and 63°C for PA6-LGF40).

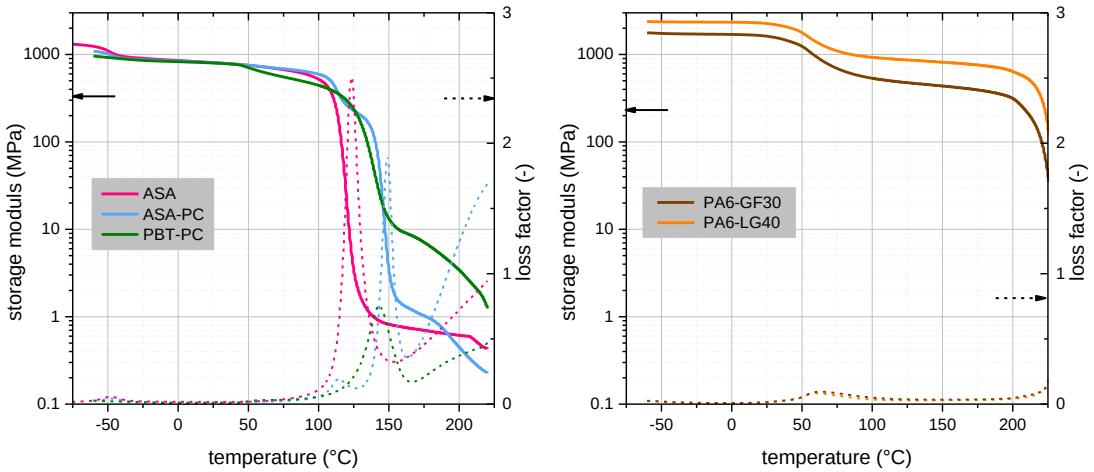

Fig. 2: Curves of the storage modulus and loss factor against temperature for unreinforced (left) and reinforced (right) plastics.

Storage moduli at the three application relevant temperatures 0°C, 23°C and 60°C are depicted in Fig. 3. Within each grade, highest moduli were obtained at 0°C. In the material comparison, at each temperature, the highest storage moduli were detected for the grade PA6-LGF40. At 60°C, the moduli of the grades ASA and ASA-PC are only moderate decreasing compared to 23°C. The PBT-PC compound shows a higher decrease, which is also visible in the DMA-curve (storage modulus against temperature) starting with diminishing storage moduli at 50°C. The reinforced grades PA6-GF30 and PA6-LGF40 exhibit a significant reduction of storage moduli between 23°C and 60°C. This is related to the immediate vicinity to the glass transition region of PA6.

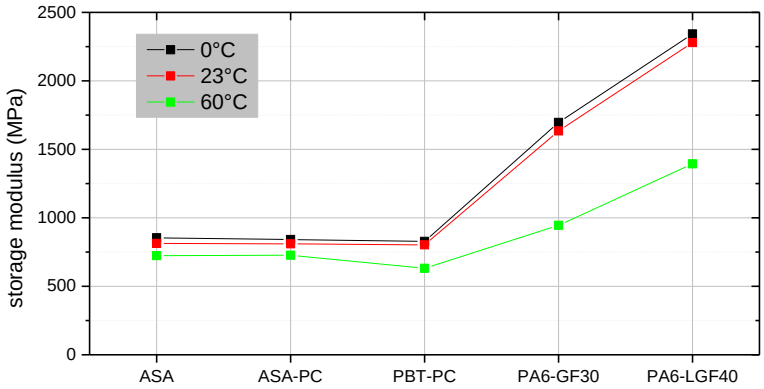

Fig. 3: Storage moduli at three different temperatures for three unreinforced and two reinforced plastics.

Temperature dependent stress-strain curves for the five plastics are plotted in Fig. 4. Based on the stress-strain curves, the values for Young's modulus, strength and strain-at-break were evaluated (see. Fig. 5). For all temperatures, the reinforced polymeric materials revealed significantly higher Young's moduli (factor 3 to 6) and strengths (factor 3 to 4). In contrast, the obtained strain-at-break values were much lower (factor 2 to 27). An increase in testing temperature led to declining Young's moduli and strengths. While the lowest values were determined for the polymer blend PBT-PC, for PA6-LGF40, the highest values were achieved. With a higher glass fiber content, an increase in Young's modulus was determined. Increasing temperatures led to higher strain-at-break values. The highest strain-at-break values were obtained for PBT-PC. For the glass fiber reinforced grades, a brittle failure and small strain-at-break values were received due to the dominating fiber influence.

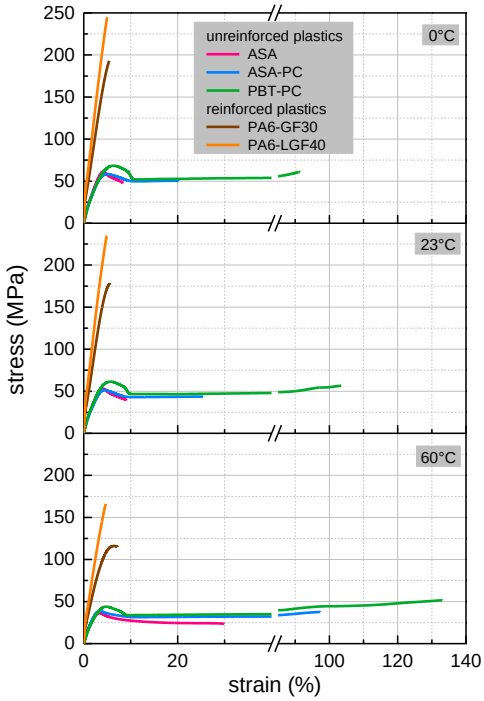

Fig. 4: Temperature dependent stress-strain curves for the three unreinforced and the two glass fiber reinforced plastics.

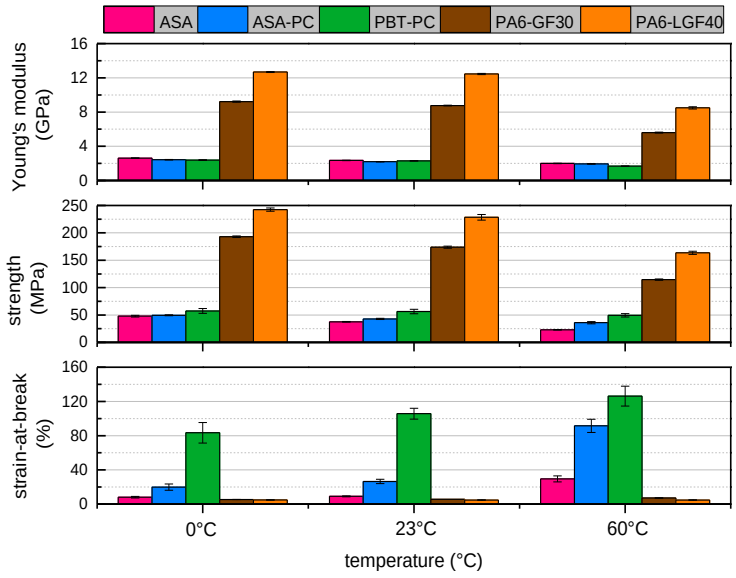

Fig. 5: Temperature dependent values of Young's modulus (top), strength (middle) and strain-at-break (bottom) for the five plastics.

In Fig. 6, the fatigue crack growth behavior of the five plastics for each testing temperature is depicted. Furthermore, the influence of different fiber orientation on the FCG resistance is revealed. For all materials, temperature increase led to a declining FCG resistance. In terms of the material comparison, for all temperatures, the glass fiber reinforced plastics revealed a significantly improved fatigue crack growth behavior. Conversely, the FCG resistance of ASA was inferior. In terms of fiber orientation, PA6-LGF40 and thus the PA grade with the long glass fiber reinforcement and the higher fiber content revealed an enhanced FCG behavior in the tests with the initial crack in mold direction. Nevertheless, tests with the initial crack in cross direction showed comparable FCG resistances for both glass fiber reinforced plastics.

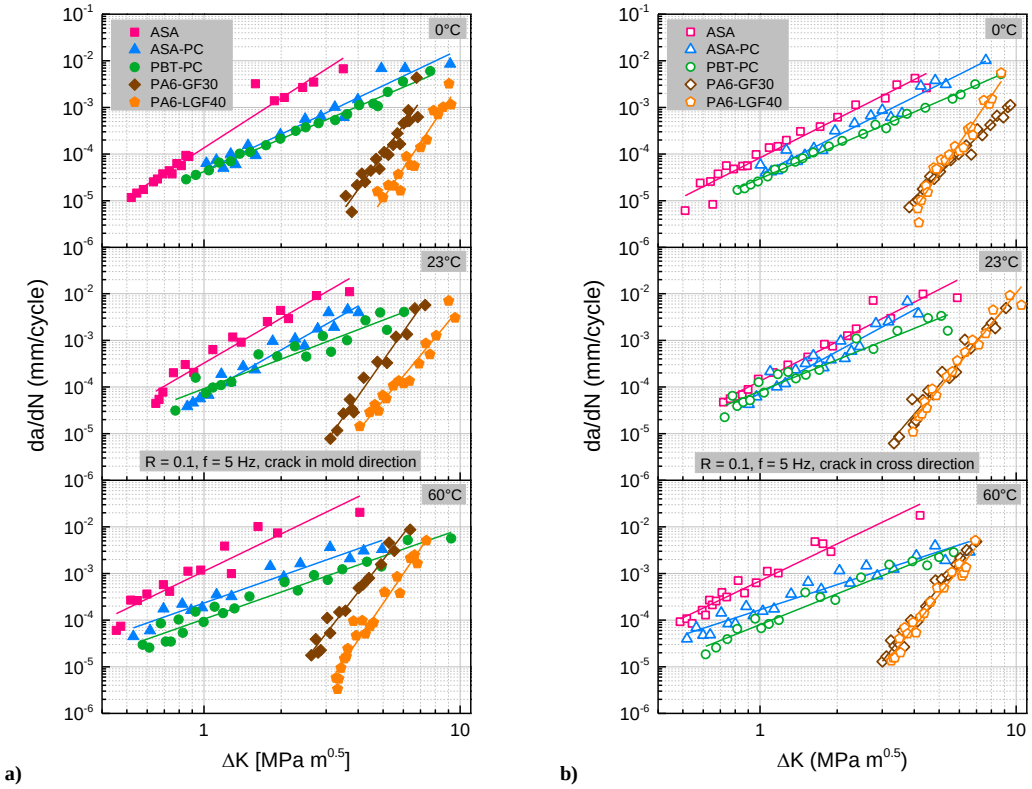

Fig. 6: Temperature dependent fatigue crack growth kinetics for the three unreinforced and the two glass fiber reinforced plastics tested with the crack in (a) mold direction and (b) cross direction.

5. Summary and conclusions

Three unreinforced and two glass fiber reinforced plastics for the application in mounting systems of solar-thermal collectors were characterized with regard to their morphological, thermomechanical, mechanical and fatigue crack growth (FCG) behavior. The three unreinforced polymeric materials included an elastomer-modified copolymer (acrylic ester-styrene-acrylonitrile, ASA) and two polymer blends (acrylic ester-styrene-acrylonitrile/polycarbonate, ASA/PC and polybutylene terephthalate/polycarbonate, PBT/PC). In the category of the reinforced materials one short glass fiber reinforced polyamide grade with a glass fiber content of 30 w% (PA6-GF30) and one long glass fiber reinforced polyamide grade with a glass fiber content of 40 w% (PA6-LGF40) were investigated. The morphological characterization revealed homogenous material distributions for all material grades. However, the polymer blend ASA/PC showed a limited miscibility leading to separated glass transition temperatures. For the three unreinforced plastics, significantly lower values for Young's modulus and strength were determined. A comparison between the strain-at-break values of the unreinforced and the reinforced plastics revealed higher values for the former materials. Decreasing Young's moduli and strengths as well as to higher strain-at-break values were detected with higher testing temperatures. At all temperatures, the reinforced plastics showed a superior FCG behavior. Increasing temperatures led to a diminishing FCG resistance. In order to investigate the effect of fiber orientation on the fatigue crack growth of the reinforced plastics, tests were carried out with specimens containing the initial crack in mold direction and in cross direction. While tests with the initial crack in cross direction revealed a similar FCG resistance, tests with the initial crack in mold direction showed a significantly better performance for the polymer with the higher fiber content.

Acknowledgement

This research work was performed in the cooperative research project *MidTempColl*. The project was funded by the Austrian Climate and Energy Fund (KLI.EN) within the program "Neue Energien 2020" and the funding was administrated by the Austrian Research Promotion Agency (FFG).

References

Altstaedt, V., 2005. The Influence of Molecular Variables on Fatigue Resistance in Stress Cracking Environments. In: Kausch HH, editor. Intrinsic molecular mobility and toughness of polymers, vol. 188. Berlin, London: Springer, pp. 105–152.

Anderson T.L.; 2017. Fracture mechanics: Fundamentals and applications. Boca Raton, FL: CRC Press.

Bradler, P.R., Fischer, J., Pohn, B., Wallner, G.M., Lang, R.W., 2017. Effect of stabilizers on the failure behavior of glass fiber reinforced polyamides for mounting and framing of solar energy applications, Energy Procedia 119, 828-834.

Bradler P.R., Fischer J., Schlaeger M, Wallner GM, Lang RW; 2016. Conference Proceedings of EuroSun 2016.

DeCoste, J.B., Malm, F.S., Wallder, V.T., 1951. Cracking of Stressed Polyethylene; Ind. Eng. Chem. 43 (1), 117-121.

Erfurth, R., Goering, J., Delzer, T., 2001. Tragkonstruktionen für Solaranlagen – Planungshandbuch zur Aufständerung von Solarkollektoren, first ed., Solarpraxis AG, Berlin, D.

Fischer, J., Bradler, P.R., Lang R.W., Wallner G.M.; 2016a. Fatigue crack growth resistance of polypropylene in chlorinated water at different temperatures, Conference Proceedings of the 18th Plastic Pipes Conference, 2016.

Fischer, J., Bradler, P.R., Schläger M.; Wallner, G.M., Lang, R.W., 2016b. Novel Solar Thermal Collector Systems in Polymer Design – Part 5; Energy Procedia; 91:27–34.

Haager M, Pinter G, Lang R.W.; 2004. Estimation of Slow Crack Growth Behavior in Polyethylene after Stepwise Isothermal Crystallization; Macromol. Symp.; 217(1):383–90.

Koehl, M., Meir, M.G., Papillon, P., Wallner, G.M., Saile, S. (Eds.), 2012. Polymeric Materials for Solar Thermal Applications, first ed., Wiley-VCH.

Lang R.W., Manson J.A., Hertzberg R.W.; 1982. Effect of short glass fibers and particulate fillers on fatigue crack propagation in polyamides; Polym. Eng. Sci.; 22(15):982–7.

Lang, R.W., Stern, A., Doerner, G., 1997. Applicability and limitations of current lifetime prediction models for thermoplastics pipes under internal pressure; Angew. Makromol. Chemie; 247(1):131–45.

Lang R.W.; 1980. Applicability of linear elastic fracture mechanics to fatigue in poymers and short-fiber composites. Dissertation. Berhlehem (US).

Lang, R.W., Pinter, G., Balika, W., 2005. Konzept zur Nachweisführung für Nutzungsdauer und Sicherheit von PE-Druckrohren bei beliebiger Einbausituation; 3R International (1-2/2005):32–41.

Schoeffl P.F., Bradler P.R., Lang R.W.; 2014. Yielding and crack growth testing of polymers under severe liquid media conditions; Polymer Testing; 40:225–33.

Schoeffl P.F., Bradler P.R., Lang R.W.; 2015. Effect of liquid oilfield-related media on slow crack growth behavior in polyethylene pipe grade materials; International Journal of Fatigue 72, 2015, 90-101.

Stern, A., Asanger, F., Lang, R.W.; 1998a. Creep crack growth testing of plastics—II. data acquisition, data reduction and experimental results. Polymer Testing 17 (6), 423–441.

Stern, A., Novotny, M., Lang, R.W.; 1998b. Creep crack growth testing of plastics—I. test configurations and test system design. Polymer Testing 17 (6), 403–422.